Research Report

Topology Optimization Method with Vector Field Design Variables

Tsuyoshi Nomura, Ercan M. Dede, Tadayoshi Matsumori and Atsushi Kawamoto

Report received on Feb. 5, 2016

ABSTRACT This report presents a topology optimization method capable of simultaneously designing both the morphology and orientation distribution of an anisotropic material. Topology optimization is a well-established structural optimization framework that optimizes the material distribution, i.e., density, in a given design domain for maximum performance. However, the optimization of structures consisting of inhomogeneously distributed anisotropic materials is still in the research phase. In this paper, a topology optimization method is extended to handle both an orientation vector distribution and a density distribution. The proposed method supports both continuous angle distribution and discrete angle set distribution using a Cartesian style orientation vector as the design variable combined with a projection method using isoparametric shape functions. The proposed method is less likely to be trapped at unwanted local optima when compared with classic continuous fiber angle optimization (CFAO), which directly uses the orientation angle as the design variable. The proposed method is built upon modern topology optimization techniques. Thus, it is versatile and flexible enough to solve multiload problems or even multiphysics problems. Singly loaded and multiply loaded stiffness maximization problems are provided as numerical examples, and the characteristics of concurrent density and orientation optimization are analyzed.

KEYWORDS Topology Optimization, Orientation Design, Isoparametric Shape Function, Projection Method, 3D Printing, Continuous Fiber Printing

1. Introduction

Topology optimization[1] is the most flexible structural optimization framework. The method optimizes the material distribution in a given design domain for maximum performance. It is well established and has been applied to many engineering problems. However, the optimization of structures consisting of inhomogeneously distributed anisotropic materials, such as composite material layout optimization, is still in the research phase.

Some of the most practical and promising anisotropic materials are fiber-reinforced composites such as carbon-fiber-reinforced plastics, CFRPs. The fiber orientation is the most important factor determining the mechanical properties of such composites. In the past, fiber orientation design for such materials was rather limited. The composite was either unidirectional or a woven fabric, and the design factor is limited to combination of these options. Currently, there are several new fabrication technologies available, such as tailored fiber placement (TFP) based on automated stitching machines,[2,3] automated fiber placement (ATP), automated tape laying (ATL), and continuous fiber printing systems[4] based on 3D printing technology. These technologies drastically expand the degree of freedom in the orientation design of anisotropic composites; however, the design methodology to elicit maximum performance from these technologies has yet to be well established. Topology optimization[1] seems to be the most promissing option to support this goal. Topology optimization was originally developed under consideration of anisotropy in material properties in the intermediate state of the optimization procedure with an anisotropic microstructure in the formulation of homogenization design method, and there has been enormous effort made for solving anisotropic topology optimization problems.[5-8] In fact, the solution of the anisotropic material layout problem has been long sought by the aerospace industry, and considerable efforts have been made using a variety of numerical strategies.[9,10] However, due to the difficulty of avoiding local optima,[7,11] a general optimization method has not yet been established, especially for the simultaneous optimization of topology and material orientation with a continuous angle distribution.

In this study, we propose a general topology

optimization method capable of the simultaneous design of topology and orientation of anisotropic materials by introducing orientation design variables in addition to the density design variable, expanding the idea of design variable projection methods.

2. Formulation

Figure 1 shows a schematic of the problem setting. In this report, we use a compliance minimization problem; that is, maximizing the stiffness of a structure, as an example problem. The topology optimization formulation starts by defining an extended design domain. In the figure, there is a rectangular domain labeled as the extended design domain D. In this setting, the extended design domain is equivalent to the analysis domain, so structural analysis can be performed on this box with certain boundary conditions, such as a supporting boundary on the left side and a load condition on the right side. Then, the design variable fields are defined in the extended design domain. Each point in the design domain may use one or more design variables to represent physical properties at that point. Usually, a design variable called density, which represents the presence of material, is assigned to each point. By defining this design variable at all points in the design domain, the design variable field is constructed. By determining the best distribution of the design variable field, the optimization algorithm attempts to find the optimal structure. In this report, we propose the introduction of an additional design variable, an orientation vector.

In the remainder of this section, the formulation of the design variable is briefly summarized, as the complete formulation was provided in a previous article by the authors.[12]

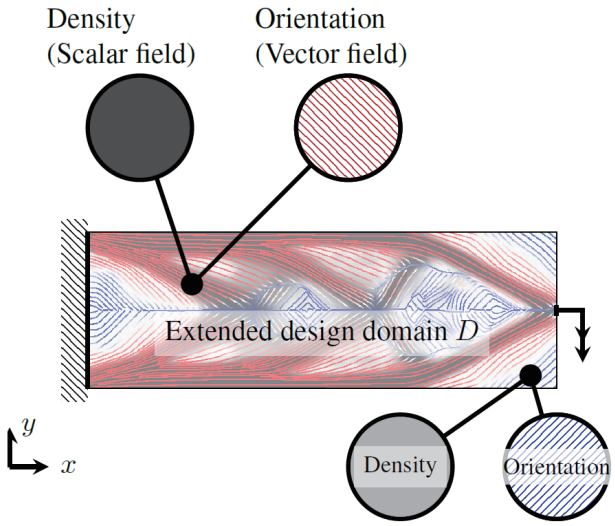

Fig. 1 Extended design domain and design variable fields.

2. 1 Topology Design

Assume that the following characteristic function $\chi(\mathbf{x})$ is defined inside D to indicate the object domain to be designed, Ω_d;

$$\chi(\mathbf{x}) = \begin{cases} 0 & \text{for } \forall \mathbf{x} \in D \setminus \Omega_d, \\ 1 & \text{for } \forall \mathbf{x} \in \Omega_d. \end{cases} \tag{1}$$

Here, $\chi(\mathbf{x})$ is defined as the Heaviside function of a precursor field, $\phi(\mathbf{x})$:

$$\chi(\mathbf{x}) = H(\phi(\mathbf{x})) = \begin{cases} 0 & \text{for } \forall \mathbf{x} \in D \setminus \Omega_d, \\ 1 & \text{for } \forall \mathbf{x} \in \Omega_d. \end{cases} \tag{2}$$

A Helmholtz filter is used[13,14] to regularize the function space as

$$-R_\phi^2 \nabla^2 \tilde{\phi} + \tilde{\phi} = \phi, \tag{3}$$

where R_ϕ is the filter radius and $\tilde{\phi}$ is a filtered field. To relax $\chi(\mathbf{x})$ to the material density field $\rho(\mathbf{x})$, the regularized Heaviside Function $\tilde{H}$ is introduced as follows:

$$\rho(\tilde{\phi}(\mathbf{x})) = \tilde{H}(\tilde{\phi}(\mathbf{x})). \tag{4}$$

The material density is used to interpolate the material properties. For a structural problem, the representative constitutive tensor, the stiffness tensor, is interpolated between void and solid state using ρ as

$$\mathbf{C}_\rho = \mathbf{C}_v + \rho^p(\mathbf{C}_s - \mathbf{C}_v), \tag{5}$$

where $\mathbf{C}_\rho$, $\mathbf{C}_v$, and $\mathbf{C}_s$ are the interpolated tensor, void tensor, and solid material tensor, respectively, and p is the density penalty parameter. In the following discussion, $\mathbf{C}_s$ is extended to anisotropic materials with a material physical parameter orientation design variable.

2. 2 Orientation Design by Isoparametric Projection

For simplicity, the discussion hereafter will focus on a two-dimensional case. A Cartesian representation is chosen for the design variable, and the orientation field in a given extended design domain is declared as follows:

$$\vartheta(\mathbf{x}) = \begin{bmatrix} \varsigma(\mathbf{x}) \\ \zeta(\mathbf{x}) \end{bmatrix}, \tag{6}$$

where

$$|\vartheta(\mathbf{x})| \leqslant 1 \quad \text{for} \quad \forall \mathbf{x} \in D. \tag{7}$$

$\upsilon(\mathbf{x})$ is a vector field with natural coordinate values ξ and η as its elements

$$\upsilon(\mathbf{x}) = \begin{bmatrix} \xi(\mathbf{x}) \\ \eta(\mathbf{x}) \end{bmatrix}, \tag{8}$$

where

$$\xi \in [-1, 1] \text{ and } \eta \in [-1, 1]. \tag{9}$$

We then define the orientation vector field as follows:

$$\vartheta(\mathbf{x}) = \mathbf{N}(\upsilon(\mathbf{x})) = \begin{bmatrix} N_x(\xi(\mathbf{x}), \eta(\mathbf{x})) \\ N_y(\xi(\mathbf{x}), \eta(\mathbf{x})) \end{bmatrix}, \tag{10}$$

where $\mathbf{N}$ is an appropriate isoparametric shape function.

Isoparametric shape functions are commonly used in the finite element method, and there are various options in choosing an isoparametric shape function, $\mathbf{N}$. Here, the eight-node bi-quadratic quadrilateral element,[15,16] also called the "serendipity" element, is used. The serendipity element is defined as follows:

$$\begin{cases} N_x(\xi, \eta) = \sum_{i=1}^{8} u_i N_i(\xi, \eta) \\ N_y(\xi, \eta) = \sum_{i=1}^{8} u_i N_i(\xi, \eta), \end{cases} \tag{11}$$

where $\mathbf{v}_i = \{u_i, v_i\}^T$ is the coordinate of the i-th node in the real coordinate system forming a unit circle, as shown in the right side image of **Fig. 2**. By changing the location of $\mathbf{v}_i = \{u_i, v_i\}^T$, the shape function can take various shapes of function value bounds. Therefore, this function can be utilized to approximate various nonlinear functions, and when the element is in the unit circle, $\|\vartheta\| \leqslant 1$ is naturally fulfilled.

The function $N_i(\xi, \eta)$ is defined as follows:

$$\begin{cases} N_1(\xi, \eta) = -(1-\xi)(1-\eta)(1+\xi+\eta)/4 \\ N_2(\xi, \eta) = \quad (1-\xi)(1-\eta)(1+\xi \quad)/2 \\ N_3(\xi, \eta) = -(1+\xi)(1-\eta)(1-\xi+\eta)/4 \\ N_4(\xi, \eta) = \quad (1+\xi)(1-\eta)(1+\eta \quad)/2 \\ N_5(\xi, \eta) = -(1+\xi)(1+\eta)(1-\xi-\eta)/4 \\ N_6(\xi, \eta) = \quad (1-\xi)(1+\eta)(1+\xi \quad)/2 \\ N_7(\xi, \eta) = -(1+\xi)(1+\eta)(1+\xi-\eta)/4 \\ N_8(\xi, \eta) = \quad (1-\xi)(1-\eta)(1+\eta \quad)/2. \end{cases} \tag{12}$$

The relationship between ϑ and υ is analogous to the relationship between $\rho(\mathbf{x})$ and $\phi(\mathbf{x})$. Similarly, a Helmholtz filter is used to regularize υ, which resides in L^∞ space projected to H^1 space. However, this time, the regularized field is a vector field

$$\tilde{\upsilon}(\mathbf{x}) = \begin{bmatrix} \tilde{\xi}(\mathbf{x}) \\ \tilde{\eta}(\mathbf{x}) \end{bmatrix}, \tag{13}$$

where υ has a box bound, Eq. (9), but $\tilde{\upsilon}$ does not have explicit bounds.

Regularization is enforced with the following equation:

$$-\mathbf{R}_\upsilon \nabla^2 \begin{bmatrix} \tilde{\xi} \\ \tilde{\eta} \end{bmatrix} + \begin{bmatrix} \tilde{\xi} \\ \tilde{\eta} \end{bmatrix} = \begin{bmatrix} \xi \\ \eta \end{bmatrix}, \tag{14}$$

where $\mathbf{R}_\upsilon = R_\upsilon^2 \mathbf{I}$, R_υ is the filter radius for the vector field, and $\mathbf{I}$ is the identity matrix. Then, unbounded $\tilde{\upsilon}$ is projected into $-1 \leqslant \tilde{\xi} \leqslant 1$, $-1 \leqslant \tilde{\eta} \leqslant 1$ in a manner similar to the $\tilde{\phi}$ to ρ projection.

$$\bar{\upsilon} = \begin{bmatrix} \bar{\xi}(\mathbf{x}) \\ \bar{\eta}(\mathbf{x}) \end{bmatrix} = \begin{bmatrix} 2\tilde{H}(\tilde{\xi}(\mathbf{x}) - 1) \\ 2\tilde{H}(\tilde{\eta}(\mathbf{x}) - 1) \end{bmatrix}. \tag{15}$$

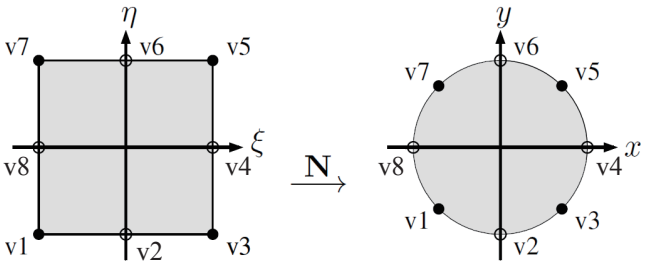

(a) Natural coordinate system (b) Real coordinate system

Fig. 2 The eight node bi-quadratic serendipity element. Left: natural coordinates. Right: real coordinates.

In concert with Eq. (10), the regularized orientation field $\tilde{\vartheta}$ is obtained as follows:

$$\tilde{\vartheta}(\mathbf{x}) = \mathbf{N}(\bar{v}(\mathbf{x})) = \begin{bmatrix} N_x(\bar{\xi}(\mathbf{x}), \bar{\eta}(\mathbf{x})) \\ N_y(\bar{\xi}(\mathbf{x}), \bar{\eta}(\mathbf{x})) \end{bmatrix} \quad \text{for } \forall \mathbf{x} \in D. \tag{16}$$

Finally, the constitutive tensor is transformed according to $\tilde{\vartheta}$

$$\mathbf{C}_a = \mathbf{C}_i + \hat{\mathbf{T}}^{-1}(\tilde{\vartheta}) \cdot (\mathbf{C}_u - \mathbf{C}_i) \cdot \hat{\mathbf{T}}'(\tilde{\vartheta}), \tag{17}$$

where $\mathbf{C}_a$ is an interpolated tensor in terms of anisotropy, $\mathbf{C}_u$ is a given unrotated anisotropic tensor, $\mathbf{C}_i$ is an isotropic component subtracted from $\mathbf{C}_u$, and $\hat{\mathbf{T}}$ and $\hat{\mathbf{T}}'$ are transformations that rotate a tensor to a direction given by ϑ; refer to the detailed description given in an earlier paper.[12]

Substituting the previous expression $\mathbf{C}_a$ into $\mathbf{C}_s$ in Eq. (5), the complete material interpolation function is finally defined as

$$\mathbf{C}(\rho, \vartheta) = \mathbf{C}_v + \rho^p(\mathbf{C}_i + \hat{\mathbf{T}}^{-1}(\tilde{\vartheta}) \cdot (\mathbf{C}_u - \mathbf{C}_i) \cdot \hat{\mathbf{T}}'(\tilde{\vartheta}) - \mathbf{C}_v). \tag{18}$$

2. 3 Optimization Problem Formulation

The general optimization problem can be formulated as follows:

$$\underset{\phi, \xi, \eta, u}{\text{minimize}} \quad F := \int_D f(\mathbf{u}) \mathrm{d}\Omega, \tag{19a}$$

$$\text{subject to} \quad \phi \in [\underline{\phi}, \bar{\phi}], \tag{19b}$$

$$\xi \in [-1, 1], \tag{19c}$$

$$\eta \in [-1, 1], \tag{19d}$$

$$g_1 := \int_D \rho \mathrm{d}\Omega - \bar{V}_f \int_D \mathrm{d}\Omega \leqslant 0, \tag{19e}$$

$$\text{Governing equations}, \tag{19f}$$

$$\text{Material interpolation}, \tag{19g}$$

where $\mathbf{u}$ is the state variable obtained from the governing equations (Eq. (19f)). In the governing equations, the material properties are coupled with the design variable fields, density (ρ), and the orientation vector (ϑ), given by (Eq. (19g)). $\bar{V}_f$ is the upper bound for the volume fraction of the material in the extended design domain.

By changing the governing equations (Eq. (19f)), this formulation can be applied to various types of physics problems, such as the thermal conduction problem[17] which uses a thermal conductivity tensor of a thermal composite as a material property, or even multiphysics problems involving electromagnetics, fluid dynamics and heat transfer[18] to optimize the orientation and density of the residual magnetic flux of a permanent magnet. In this report, we use elastic equilibrium governing equations (Eq. (19f)) as follows:

$$\begin{aligned} -\nabla \cdot \boldsymbol{\sigma} &= 0 \quad \text{in } D, \\ \mathbf{u} &= 0 \quad \text{on } \partial D_u, \\ \boldsymbol{\sigma} \cdot \mathbf{n} &= t \quad \text{on } \partial D_t. \end{aligned} \tag{20}$$

By assuming plane stress conditions, the constitutive laws can be described as

$$\boldsymbol{\sigma} = \mathbf{C}(\rho, \vartheta) \cdot \boldsymbol{\epsilon}, \tag{21}$$

where $\boldsymbol{\epsilon} = \left[\frac{\partial u_1}{\partial x_1} \ \frac{\partial u_2}{\partial x_2} \ \frac{1}{2}\left(\frac{\partial u_1}{\partial x_2} + \frac{\partial u_2}{\partial x_1} \right) \right]^T$.

The objective function for the compliance minimization problem is

$$F = \int_D W_s \mathrm{d}\Omega, \tag{22}$$

where $W_s = \boldsymbol{\sigma}\boldsymbol{\epsilon}/2$ is the strain energy density.

3. Numerical Examples

3. 1 Single Load Cantilever

A short cantilever benchmark problem is solved, in which the left side (∂D_u) is fixed and the middle of the right side ($\partial \Omega_t$) is subjected to surface loading. The analysis geometry and boundary condition settings are as shown in **Fig. 3**. A $w_c \times h_c$ rectangular domain is given as the analysis domain, and the entire area is designated as an extended design domain, D. The geometric parameters w_c and h_c are 3 and 1, respectively. The $-y$ direction surface load t on ∂D_t is set to unity, and the length of ∂D_t is $h_c/10$. A square grid mesh with a side length of $d = 0.02$ is used in combination with Lagrange linear quadrilateral elements. The upper bound of the volume fraction, $\bar{V}_f$, is set to 0.5.

Two algorithms are tested. One is concurrent

optimization, which optimizes the density and orientation fields simultaneously, and the other is serial optimization, which optimizes the density field first and then optimizes the orientation field using a fixed optimized density field.

Figure 4 shows the obtained design solution. The figure shows seven configurations at various iteration steps to depict the evolution of the topology and orientation distribution by the proposed method. The gray scale image in the background shows the topology density, the streamlines show the direction of the orientation vector, and the color of the streamlines show the norm of the orientation vector. The blue streamlines show that the orientation vector has a small norm, and therefore a weak orientation, whereas the red streamlines show that the orientation is strongly defined to the streamline direction.

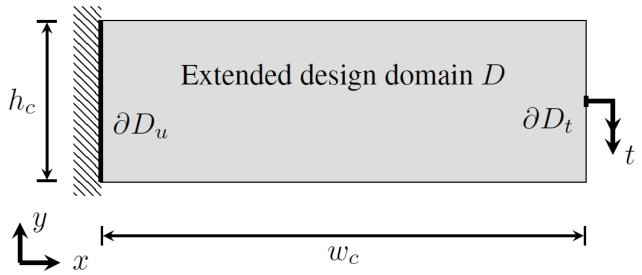

Fig. 3 Geometry settings for the short cantilever problem.

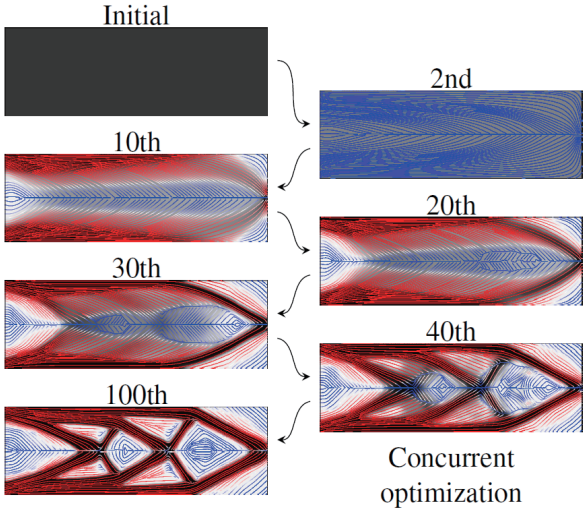

Fig. 4 Optimization results for the short cantilever problem with a volume fraction of 0.5 using a concurrent optimization scheme at various iteration steps. The gray scale image, the streamline, and the color of the streamline indicate the density, orientation direction, and norm of the orientation vector (blue: weak orientation, red: strong orientation), respectively.

At the beginning, indicated as "initial" in the figure, the orientation vector design variable is uniform, so there is no streamline. At the second iteration, the streamlines appear along the principal stress direction of the rectangular cantilever. At the 10th iteration step, a non-uniform distribution of the density and orientation vector norm is recognized, but it is still smooth except for the middle line and there is no large change in topology. At the 20th iteration step, a site with different orientation direction is generated in the low density are of the beam center. At the 30th iteration step, the number of discontinuous angle sites increases, and a hole is initiated at the tip of the cantilever. At the 40th iteration step, the topology evolves to a double-cross configuration and the orientation distribution shows more complexity. Finally, at the 100th iteration, the topology becomes clear and the fiber reinforcement orientation angle is aligned with the small bars comprising the cantilever structure. Note that the orientation vector smoothly rotates as the topology progresses, and sometimes the change of the fiber orientation angle occurs prior to the topological change.

Figure 5 shows the optimal configuration obtained by isotropic optimization on the left and serial optimization on the right. Since this is a single-load problem, the configuration obtained by the concurrent optimization is almost identical to that obtained by the serial optimization, supporting the empirical knowledge that the optimal orientation should coincide with the principal stress direction.

3. 2 Multiload Cantilever

In the previous example, even though some interaction between the density evolution and orientation evolution is observed, the obtained topology is very similar to the results of ordinary topology optimization that only takes the density into account. However, in more complex situations

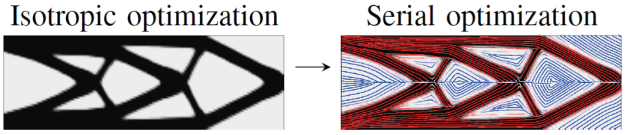

Fig. 5 Results of isotropic and serial optimization.

such as multiload cases, multiphysics[18] or alternative physics problems,[17] we may find the simultaneous optimization of topology and orientation more beneficial.

Here, we extend the problem to multiply loaded cases. **Figure 6** shows the problem setting. The analysis domain and boundary conditions are almost identical to the previous case, but two load cases are applied in this setting. The first is exactly the same load conditions as were applied to the previous example; that is, a vertical load is applied to the center of the right end of the cantilever ∂D_t, depicted as t_1 in the figure. The second is applied at the same location ∂D_t but horizontally, depicted as t_2. The two load cases are analyzed independently, and various combinations of load ratio and volume fraction are analyzed and optimized.

The objective function F_m is formulated as follows:

$$F_m = r_l F_1 + (1 - r_l) F_2, \tag{23}$$

where r_l, $(0 \leqslant r_l \leqslant 1)$ is called the load ratio, and is a weighting factor for the objective function values calculated for each load case. Both concurrent and serial optimization algorithms are tested for each case.

Figures 7 through **9** show comparisons between concurrent optimization and serial optimization for various combinations of load ratio and volume fraction, and **Fig. 10** shows a plot of the objective function. In general, concurrent optimization tends to yield structures with a fewer members and holes. Contrarily, the configurations obtained by serial optimization are more complex. The difference in the objective is not very large. The maximum difference is about 10%, and lower load ratios and smaller volume fractions tend to result in larger differences.

One reason for this behavior may be that serial optimization determines topology using only the

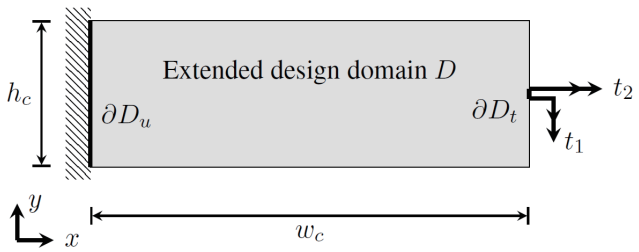

Fig. 6 Geometry settings for the multiload cantilever problem.

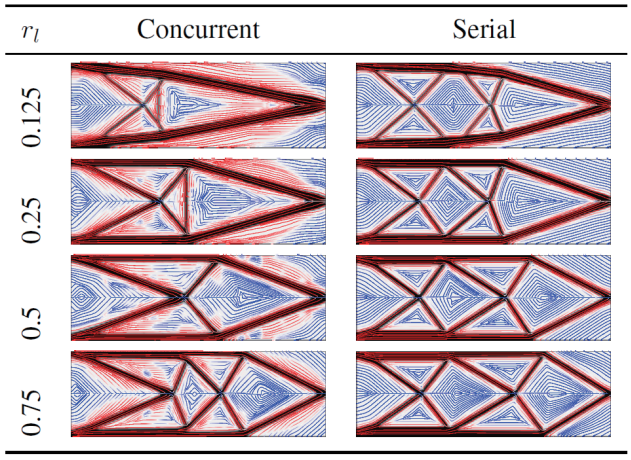

Fig. 7 Optimized configurations for the multiload cantilever problem (volume fraction $V_f = 0.25$).

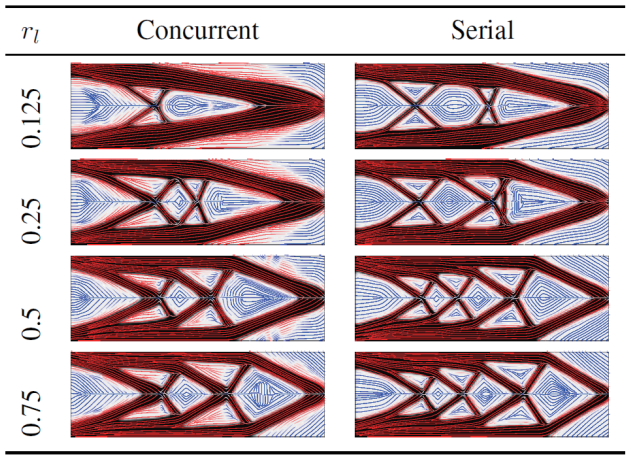

Fig. 8 Optimized configurations for the multiload cantilever problem (volume fraction $V_f = 0.5$).

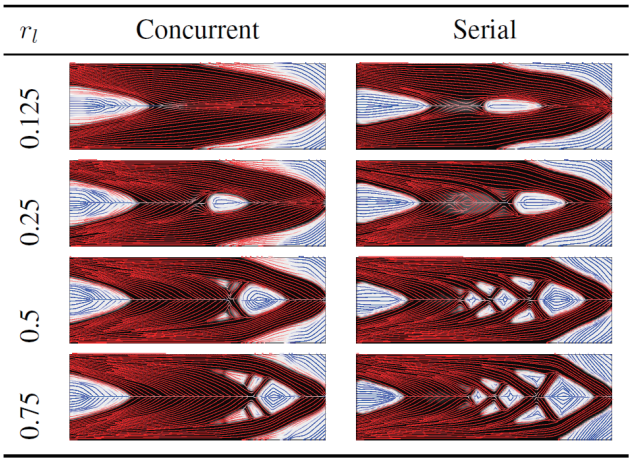

Fig. 9 Optimized configurations for the multiload cantilever problem (volume fraction $V_f = 0.75$).

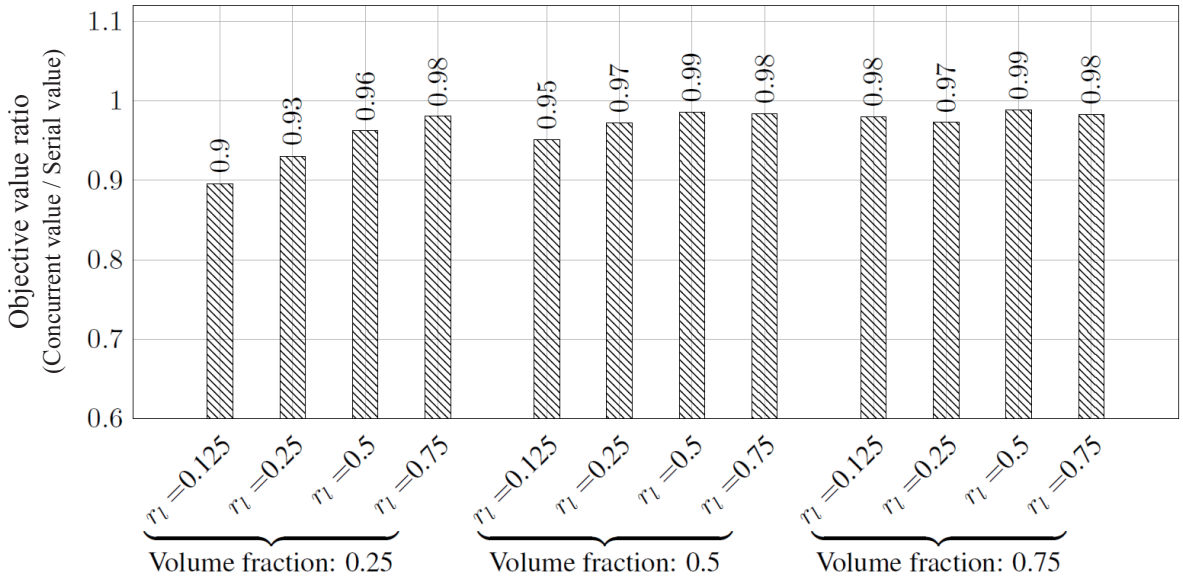

Fig. 10 Objective value ratio for multiload cantilever problem.

density field, so it involves only single Helmholtz filtering. On the other hand, concurrent optimization involves three Helmholtz filters for optimization, inducing topological changes. Figure 10 shows that the objective function ratio is always less than 1. That means that concurrent optimization always finds a better solution than serial optimization. This result is interesting because usually more complex structures have a lower compliance in compliance minimization problems with isotropic materials. This suggests that, depending on the loading conditions, serial optimization risks missing optimal structures that can be found with concurrent optimization.

4. Conclusion

A topology optimization method capable of the simultaneous design of topology and orientation using an isoparametric projection method was proposed. The method is based on density filter topology optimization methods, and an orientation vector is used to represent orientation along with a projection method using isoparametric shape functions. Numerical experiments were performed with compliance minimization problems involving both singly loaded and multiply loaded short cantilevers. Concurrent optimization, which simultaneously optimizes the density and orientation fields, and serial optimization, which optimizes the density field first and then optimizes the orientation field using a fixed optimized density field, are compared. The results reveal that both methods yield almost identical results for singly loaded cases, but in multiply loaded cases concurrent optimization could have better performance, depending on the load case.

Acknowledgments

This work was partially supported by Council for Science, Technology and Innovation (CSTI); New Energy and Industrial Technology Development Organization (NEDO); Cross-Ministerial Strategic Innovation Promotion Program (SIP), Innovative design/manufacturing technologies.

References

(1) Bendsøe, M. P. and Kikuchi, N., “Generating Optimal Topologies in Structural Design Using a Homogenization Method”, *Comput. Methods Appl. Mech. Eng.*, Vol. 71 (1988), pp. 197-224.
(2) Mattheij, P., Gliesche, K. and Feltin, D., “Tailored Fiber Placement-mechanical Properties and Applications”, *J. Reinf. Plast. Compos.*, Vol. 17, No. 9 (1998), pp. 774-786.
(3) Uhlig, K., Spickenheuer, A., Bittrich, L. and Heinrich, G., “Development of a Highly Stressed Bladed Rotor Made of a CFRP Using the Tailored Fiber Placement Technology”, *Mech. Compos. Mater.*, Vol. 49, No. 2 (2013), pp. 201-210.

(4) Namiki, M., Ueda, M., Todoroki, A., Hirano, Y. and Matsuzaki, R., "3D Printing of Continuous Fiber Reinforced Plastic", *SAMPE J.* (2014), p. 6.
(5) Pedersen, P., "Examples of Density, Orientation, and Shape-optimal 2D-design for Stiffness and/or Strength with Orthotropic Materials", *Struct. Multidiscipl. Optim.*, Vol. 26, No. 1-2 (2004), pp. 37-49.
(6) Zhou, K. and Li, X., "Topology Optimization for Minimum Compliance under Multiple Loads Based on Continuous Distribution of Members", *Struct. Multidiscipl. Optim.*, Vol. 37, No. 1 (2008), pp. 49-56.
(7) Stegmann, J. and Lund, E., "Discrete Material Optimization of General Composite Shell Structures", *Int. J. Numer. Methods Eng.*, Vol. 62, No. 14 (2005), pp. 2009-2027.
(8) Gao, T., Zhang, W. and Duysinx, P., "A Bi-value Coding Parameterization Scheme for the Discrete Optimal Orientation Design of the Composite Laminate", *Int. J. Numer. Methods Eng.*, Vol. 91, No. 1 (2012), pp. 98-114.
(9) Vanderplaats, G. N., "Structural Optimization: Past, Present, and Future", *AIAA J.*, Vol. 20, No. 7 (1982), pp. 992-1000.
(10) Harris, C. E., Starnes, J. H. and Shuart, M. J., "Design and Manufacturing of Aerospace Composite Structures, State-of-the-art Assessment." *J. Aircr.*, Vol. 39, No. 4 (2002), pp. 545-560.
(11) Ansola, R., Canales, J., Tarrago, J. and Rasmussen, J., "On Simultaneous Shape and Material Layout Optimization of Shell Structures", *Struct. Multidiscipl. Optim.*, Vol. 24, No. 3 (2002), pp. 175-184.
(12) Nomura, T., Dede, E. M., Lee, J., Yamasaki, S., Matsumori, T., Kawamoto, A. and Kikuchi, N., "General Topology Optimization Method with Continuous and Discrete Orientation Design Using Isoparametric Projection", *Int. J. Numer. Methods Eng.*, Vol. 101, No. 8 (2015), pp. 571-605.
(13) Kawamoto, A., Matsumori, T., Yamasaki, S., Nomura, T., Kondoh, T. and Nishiwaki, S., "Heaviside Projection Based Topology Optimization by a PDE-filtered Scalar Function", *Struct. Multidiscipl. Optim.*, Vol. 44, No. 1 (2011), pp. 19-24.
(14) Lazarov, B. S. and Sigmund, O., "Filters in Topology Optimization Based on Helmholtz-type Differential Equations", *Int. J. Numer. Methods Eng.*, Vol. 86, No. 6 (2011), pp. 765-781.
(15) Ergatoudis, I., Irons, B. and Zienkiewicz, O., "Curved, Isoparametric, 'Quadrilateral' Elements for Finite Element Analysis", *Int. J. Solids Struct.*, Vol. 4, No. 1 (1968), pp. 31-42.
(16) Arnold, D. and Awanou, G., "The Serendipity Family of Finite Elements", *Found. Comut. Math.*, Vol. 11, No. 3 (2011), pp. 337-344.
(17) Dede, E. M., Nomura, T. and Lee, J., "Thermal-composite Design Optimization for Heat Flux Shielding, Focusing, and Reversal", *Struct. Multidiscipl. Optim.*, Vol. 49, No. 1 (2013), pp. 59-68.
(18) Lee, J., Nomura, T. and Dede, E. M., "Heat Flow Control in Thermo-magnetic Convective Systems Using Engineered Magnetic Fields", *Appl. Phys. Lett.*, Vol. 101, No. 12 (2012), 123507.

Fig. 2
Reprinted from Int. J. Numer. Methods. Eng., Vol. 101, No. 8 (2015), pp. 571-605, Nomura, T., Dede, E. M., Lee, J., Yamasaki, S., Matsumori, T., Kawamoto, A. and Kikuchi, N., General Topology Optimization Method with Continuous and Discrete Orientation Design Using Isoparametric Projection, © 2014 John Wiley & Sons, Ltd., with permission from John Wiley and Sons.

Tsuyoshi Nomura
Research Field:
- Topology Optimization

Academic Degree: Ph.D.
Academic Society:
- The Japan Society of Mechanical Engineers

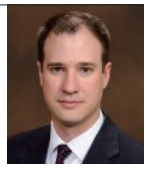

Ercan M. Dede*
Research Fields:
- Topology Optimization
- Thermal Management

Academic Degree: Ph.D.
Academic Society:
- The American Society of Mechanical Engineers

Awards:
- ASME InterPACK, Outstanding Paper Award, 2015
- R&D 100 Award, 2013
- ASME EPPD, Journal of Electronic Packaging, Best Paper Awards, 2012 and 2013

Tadayoshi Matsumori
Research Fields:
- Optimum Design
- Topology Optimization
- Shape Optimization

Academic Degree: Ph.D.
Academic Society:
- The Japan Society of Mechanical Engineers

Award:
- JSME Merit for Best Technological Presentation, 2009

Atsushi Kawamoto
Research Fields:
- Topology Optimization
- Nonlinear Dynamics
- Math Programming

Academic Degree: Ph.D.
Academic Society:
- The Japan Society of Mechanical Engineers

Award:
- JSME Design & Systems Achievement Award, 2014

* Toyota Research Institute of North America

